

---

# TDMPBC: SELF-IMITATIVE REINFORCEMENT LEARNING FOR HUMANOID ROBOT CONTROL

---

Zifeng Zhuang<sup>1\*</sup> Diyuan Shi<sup>1\*</sup> Runze Suo<sup>1</sup> Xiao He<sup>1</sup> Hongyin Zhang<sup>1</sup>  
 Ting Wang<sup>1†</sup> Shangke Lyu<sup>1†</sup> Donglin Wang<sup>1†</sup>

<sup>1</sup>Westlake University \*Equal Contribution †Corresponding Authors

## ABSTRACT

Complex high-dimensional spaces with high Degree-of-Freedom and complicated action spaces, such as humanoid robots equipped with dexterous hands, pose significant challenges for reinforcement learning (RL) algorithms, which need to wisely balance exploration and exploitation under limited sample budgets. In general, feasible regions for accomplishing tasks within complex high-dimensional spaces are exceedingly narrow. For instance, in the context of humanoid robot motion control, the vast majority of space corresponds to falling, while only a minuscule fraction corresponds to standing upright, which is conducive to the completion of downstream tasks. Once the robot explores into a potentially task-relevant region, it should place greater emphasis on the data within that region. Building on this insight, we propose the **Self-Imitative Reinforcement Learning (SIRL)** framework, where the RL algorithm also imitates potentially task-relevant trajectories. Specifically, trajectory return is utilized to determine its relevance to the task and an additional behavior cloning is adopted whose weight is dynamically adjusted based on the trajectory return. As a result, our proposed algorithm achieves 120% performance improvement on the challenging HumanoidBench with 5% extra computation overhead. With further visualization, we find the significant performance gain does lead to meaningful behavior improvement that several tasks are solved successfully.

## 1 Introduction

Humanoid robots with dexterous hands have vast and promising application scenarios due to their behavior flexibility and human-like morphology [Bonci et al., 2021, Stasse and Flayols, 2019, Choudhury et al., 2018]. Unfortunately, such complex high-dimensional space is extremely challenging for policy learning with online reinforcement learning (RL) [Sferrazza et al., 2024, Peters et al., 2003], which interactively explores the environment and learns optimal decision-making from scratch under the guidance of reward function. This paradigm has achieved significant success in fields like gaming AI [Silver et al., 2016, 2017, Schrittwieser et al., 2020, Hessel et al., 2018] and quadrupedal robots control [Miki et al., 2022, Lee et al., 2020, Hwangbo et al., 2019]. But when facing humanoid robots equipped with dexterous hands, existing RL methods struggle to learn effectively and efficiently. Even sample-efficient model-based state-of-the-art (SOTA) algorithms, such as TD-MPC2 [Hansen et al., 2023] and DreamerV3 [Hafner et al., 2023], perform poorly in humanoid control.

In high-dimensional complex spaces, the regions capable of accomplishing tasks are typically exceedingly narrow and difficult to explore compared to the entire space. For humanoid robot motion control, upright posture is a prerequisite to com-

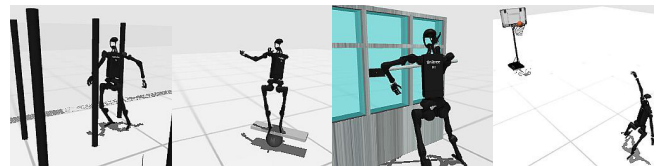


Figure 1: Tasks accomplished by TDMPBC: 1) navigating through pole-filled areas by staying close to the wall, 2) maintain balance on unstable board with the spherical pivot beneath the board in motion, 3) window cleaning with arm-controlled cleaning tools and 4) achieving a successful basketball shot.

plete any downstream tasks. Maintaining an upright posture is similar to balancing an inverted pendulum, where only an extremely small vertical region within the entire space can sustain this posture, while other regions lead to rapid falls. Therefore, when the algorithm explores an upright posture, the humanoid robot should place particular emphasis on it.

Furthermore, upright posture can be intuitively reflected in return. Only if the current timestep maintains an upright posture is it possible to continue obtaining rewards in the following timesteps. If the current step results in a fall, given that humanoid robots are virtually incapable of standing up after

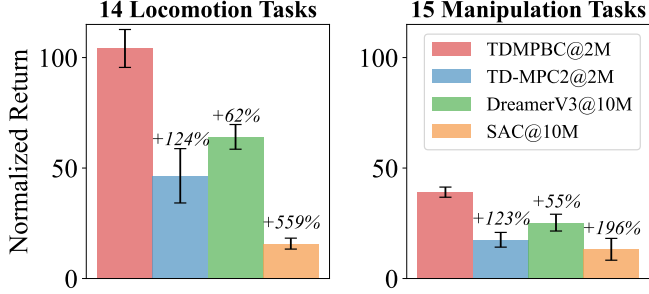


Figure 2: Performance of TDMPBC with 2M interaction steps compared to the baselines TD-MPC2 with 2M, DreamerV3 with 10M and SAC with 10M on HumanoidBench.

falling, subsequent rewards become unattainable. Under the cumulative effect, the ability to maintain an upright posture will ultimately be reflected very prominently in the return. To summarize, the return can be approximated as an indicator of whether the humanoid robot has entered a task-completing region in its control.

Based on the above observation and analysis, we propose a framework called **Self-Imitative Reinforcement Learning (SIRL)** to assist online learning in complex high-dimensional humanoid robot control. Building upon the foundation of RL algorithms, SIRL additionally imitates trajectories with high returns. This enables the humanoid robot to quickly learn the upright posture, thereby accelerating the completion of downstream tasks. Specifically, we augment the policy training objective in TD-MPC2 [Hansen et al., 2023, 2022a] with an additional behavior cloning term whose weight is dynamically adjusted based on the trajectory return. Since the trajectories being imitated are generated by the algorithm itself during exploration, rather than expert demonstrations as in traditional imitation learning (IL), our framework is termed self-imitative. Additionally, we refer to TD-MPC2 augmented with a behavior cloning loss as TDMPBC.

We have validated our proposed TDMPBC on HumanoidBench [Sferrazza et al., 2024] which contains 31 challenging tasks for the Unitree H1 robot with dexterous hands. Compared with the baseline TD-MPC2, our proposed method achieves an approximate increase more than 120% for the normalized return<sup>1</sup>. What’s more, our method enjoys a significantly faster convergence rate and excels in terms of sample-efficiency. In humanoid locomotion tasks, our algorithm is capable of completing 8 tasks out of 14 with only 2M training steps, whereas the baseline could only accomplish 1 task.

## 2 Preliminaries

**Reinforcement Learning** Reinforcement Learning (RL) is a framework of sequential decision. Typically, this problem is formulated by a Markov Decision Process (MDP)

<sup>1</sup>We normalize the return to the range  $[0, R_{\text{target}}]$ . For the push and package manipulation tasks, where the return may be negative, we do not display them in Figure 2. The performance of TDMPBC on these two tasks is on par with the baseline, which does not affect the above conclusions we have drawn.

$\mathcal{M} = \{\mathcal{S}, \mathcal{A}, r, p, d_0, \gamma\}$ , with state space  $\mathcal{S}$ , action space  $\mathcal{A}$ , scalar reward function  $r$ , transition dynamics  $p$ , initial state distribution  $d_0(s_0)$  and discount factor  $\gamma$  [Sutton et al., 1998]. The objective of RL is to learn a policy  $\pi(\mathbf{a}_t | \mathbf{s}_t)$  at timestep  $t$ , where  $\mathbf{a}_t \in \mathcal{A}$  and  $\mathbf{s}_t \in \mathcal{S}$ . Given this definition, the distribution of trajectory  $\tau = (s_0, \mathbf{a}_0, \dots, s_H, \mathbf{a}_H)$  generated by the interaction with the environment  $\mathcal{M}$  is  $P_\pi(\tau) = d_0(s_0) \prod_{t=0}^{T-1} \pi(\mathbf{a}_t | \mathbf{s}_t) p(\mathbf{s}_{t+1} | \mathbf{s}_t, \mathbf{a}_t)$ , where  $T$  is the length of the trajectory and can be infinite. Then, the goal of RL can be written as an expectation under the trajectory distribution  $J(\pi) = \mathbb{E}_{\tau \sim P_\pi(\tau)} \left[ \sum_{t=0}^T \gamma^t r(\mathbf{s}_t, \mathbf{a}_t) \right]$ . This objective can also be measured by a value function  $Q_\pi(s, \mathbf{a})$ , the expected discounted return given the action  $\mathbf{a}$  in state  $s$ :  $Q_\pi(s, \mathbf{a}) = \mathbb{E}_{\tau \sim P_\pi(\tau | s, \mathbf{a})} \left[ \sum_{t=0}^T \gamma^t r(\mathbf{s}_t, \mathbf{a}_t) | s_0 = s, \mathbf{a}_0 = \mathbf{a} \right]$ .

**TD-MPC2** Model-based RL algorithm TD-MPC2 learns a latent decoder-free world model and selects actions during inference via planning with learned model [Hansen et al., 2023]. Specifically, TD-MPC2 consists of five components:

State Encoder:	$\mathbf{z}_t = h_\phi(\mathbf{s}_t)$ ,
Latent Dynamics:	$\mathbf{z}_{t+1} = d_\phi(\mathbf{z}_t, \mathbf{a}_t)$ ,
Reward Function:	$\hat{r}_t = R_\phi(\mathbf{z}_t, \mathbf{a}_t)$ ,
Value Function:	$\hat{q}_t = Q_\phi(\mathbf{z}_t, \mathbf{a}_t)$ ,
Policy Prior:	$\hat{\mathbf{a}}_t \sim \pi_\theta(\cdot   \mathbf{z}_t)$ ,

where  $\mathbf{s}_t$  is the states,  $\mathbf{a}_t$  is the actions and  $\mathbf{z}_t$  is the latent representation. The encoder  $h_\phi$ , dynamics  $d_\phi$ , reward  $R_\phi$ , value  $Q_\phi$  compose the world model in TD-MPC2 that is trained by minimizing the following objective:

$$\mathcal{L}(\phi) = \mathbb{E}_{(\mathbf{s}_t, \mathbf{a}_t, r_t, \mathbf{s}_{t+1})_{t=0}^H \sim \mathcal{B}} \left[ \sum_{t=0}^H \lambda^t \left( l_d^{(t)} + l_r^{(t)} + l_q^{(t)} \right) \right],$$

$$l_d^{(t)} = \|d_\phi(\mathbf{z}_t, \mathbf{a}_t) - \bar{\mathbf{z}}_{t+1}\|_2^2,$$

$$l_r^{(t)} = \text{CE} \left[ R_\phi(\mathbf{z}_t, \mathbf{a}_t) - r_t \right],$$

$$l_q^{(t)} = \text{CE} \left[ Q_\phi(\mathbf{z}_t, \mathbf{a}_t) - \left( r_t + \gamma Q_{\bar{\phi}}(\mathbf{z}_{t+1}, \pi_\theta(\cdot | \mathbf{z}_{t+1})) \right) \right],$$

where  $(\mathbf{s}_t, \mathbf{a}_t, r_t, \mathbf{s}_{t+1})_{t=0}^H$  is a trajectory with length  $H$  sampled from the replay buffer  $\mathcal{B}$ ,  $\bar{\mathbf{z}}_{t+1} = h_{\bar{\phi}}(\mathbf{s}_{t+1})$  is the target latent representation and CE is the cross-entropy loss. The policy prior  $\pi$  is a stochastic maximum entropy policy that learns to maximize the objective:

$$\mathcal{L}(\theta) = \mathbb{E}_{\mathbf{s}_{t=0}^H \sim \mathcal{B}} \left[ \sum_{t=0}^H \lambda^t \left[ Q_\phi(\mathbf{z}_t, \pi_\theta(\cdot | \mathbf{z}_t)) - \alpha \mathcal{H}(\pi(\cdot | \mathbf{z}_t)) \right] \right],$$

where  $\mathcal{H}$  is the entropy of policy  $\pi$  and the parameter  $\alpha$  can be automatically adjusted based on an entropy target [Haarnoja et al., 2018] or moving statistics [Hafner et al., 2023].

During inference, TD-MPC2 plan actions using a sampling-based planner Model Predictive Path Integral (MPPI) [Williams et al., 2015] to iteratively fits a time-dependent multivariate Gaussian with diagonal covariance over the trajectory space

such that the estimated return  $\hat{\mathcal{R}}$  is maximized:

$$\hat{\mathcal{R}} = \sum_{t=0}^{H-1} \gamma^t R_\phi(\mathbf{z}_t, \mathbf{a}_t) + \gamma^H Q_\phi(\mathbf{z}_t, \mathbf{a}_t). \quad (1)$$

To accelerate this planning, a fraction of trajectories are generated by the learned policy prior  $\pi_\theta$ .

**Imitation Learning** In Imitation Learning (IL) [Zare et al., 2024], the ground truth reward is not observed and only a set of demonstrations  $\mathcal{D} = \{(\mathbf{s}_t, \mathbf{a}_t)\}$  collected by the expert policy is provided. The goal of IL is to recover a policy that matches the expert. Behavior cloning [Pomerleau, 1988] is the most simple and straightforward approach

$$\pi_{\text{BC}} = \underset{\pi}{\operatorname{argmax}} \mathbb{E}_{(\mathbf{s}_t, \mathbf{a}_t) \sim \mathcal{D}} [\log \pi(\mathbf{a}_t | \mathbf{s}_t)].$$

### 3 Self-Imitative Reinforcement Learning

In this section, we first highlight the relationship between the motion control of humanoid robots and the upright posture. We further observe that maintaining an upright posture corresponds to higher returns. Building on this insight, we introduce **Self-Imitative Reinforcement Learning (SIRL)** and present the implementation based on the model-based algorithm TD-MPC2 [Hansen et al., 2023]. During the online reinforcement learning process, **SIRL** provides additional guidance to the humanoid robot to imitate trajectories with high returns. Finally, we analyze the characteristics and applicability of this framework from multiple perspectives.

#### 3.1 Motivation and Analysis

In humanoid robot motion control, stable upright posture is the essential foundation for both locomotion tasks and whole-body manipulation tasks. This point is not only intuitive but also can be reflected in the design of the reward function. For example, in Isaac Lab, the reward term related to maintaining upright posture is assigned one extremely high weight:

$$r_1 = 200 \times r_{\text{upright}} + 1.0 \times r_{\text{velocity}} + \dots, \quad (2)$$

where  $r_{\text{upright}}$  represents an abstraction of all the reward terms associated with maintaining an upright posture, rather than a specific reward term. While the term  $r_{\text{velocity}}$  rewards velocity tracking. When tracking different desired velocities, such as 0 m/s, 1 m/s and 5 m/s, each corresponds to distinct tasks, namely stand, walk, and run.

Other reward terms are omitted for simplicity. In other environments, such as HumanoidBench [Sferrazza et al., 2024], the upright term  $r_{\text{upright}}$  serves as a weight to affect the value of the entire reward function:

$$r_2 = r_{\text{upright}} \times (r_{\text{velocity}} + \dots). \quad (3)$$

Here  $r_{\text{upright}} \in [0, 1]$ . Intuitively, the upright state with  $r_{\text{upright}} = 1$  should only occupy an extremely narrow region in the whole state-action space. In contrast, the vast majority of the space belongs to  $r_{\text{upright}} = 0$ . Therefore, once the algorithm explores into the region where an upright posture can be maintained, it

should place particular emphasis on it. After all, maintaining an upright posture facilitates further exploration and learning for downstream tasks. The next question is how to determine whether the upright posture has been explored in the control tasks of humanoid robots.

In reality, for humanoid robots, only standing upright  $r_{\text{upright}} = 1$  and falling down  $r_{\text{upright}} = 0$  are stable states. Other postures, such as  $r_{\text{upright}} = 0.6$ , will eventually evolve into the stable state of falling. Moreover, once a humanoid robot falls, it cannot recover to a standing state on its own, which means that subsequent rewards become unattainable. Under the cumulative effect, the ability to maintain a stable standing posture will ultimately be very prominently reflected in the return. We further illustrate this phenomenon with the following example.

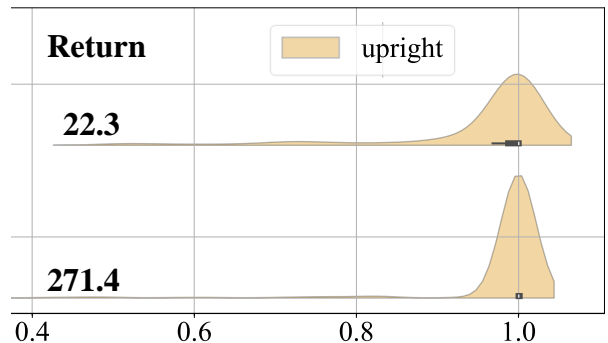


Figure 3: The first row presents the return mean of the trajectories obtained by evaluating the policy trained for 100000 steps on the task run, along with the violin plot distribution of  $r_{\text{upright}}$  across all timesteps. The second row shows the results obtained after training for 300000 steps.

From the Figure 3, we observe that the distribution of  $r_{\text{upright}}$  obtained from policies trained for 100000 and 300000 steps exhibit relatively small differences. But the final returns show a significant disparity (22.3 v.s. 271.4). This discrepancy arises because minor differences in whether the humanoid remains upright at each timestep are cumulatively amplified over multiple timesteps.

Overall, the motion control of humanoid robots is closely related to maintaining an upright posture, and whether or not the robot remains upright can lead to a substantial difference in final return. Based on this finding, an idea for accelerating or assisting humanoid robots emerges: during the online reinforcement learning (RL) exploration process, we can provide additional guidance to the robot to imitate trajectories with high returns. This approach enables the robot to first learn how to maintain an upright posture, which then serves as a foundation for completing the entire task.

#### 3.2 Framework and Methods

Now we introduce the concept of Self-Imitative Reinforcement Learning (SIRL) which aims to accelerate the learning process of humanoid robots. During the online exploration process, in addition to the basic RL loss, the policy  $\pi_\theta$  is also required

to imitate trajectories with high returns stored in the replay buffer. Unlike classical imitation learning, where trajectories are typically provided by an expert, the trajectories imitated here are generated by the policy **itself**. That is why we call the framework as “self-imitative”.

We have implemented the SIRL framework based on the TD-MPC2 algorithm [Hansen et al., 2023]. Specifically, only the policy training loss function is modified and the difference is highlighted by **red**:

$$\mathcal{L}_\pi(\theta) = \mathbb{E}_{(s_t, \mathbf{a}_t, R_t)_{t=0}^H \sim \mathcal{B}} \left[ \sum_{t=0}^H \lambda^t \left[ \underbrace{\omega(R_t) \cdot \log \pi_\theta(\mathbf{a}_t | \mathbf{z}_t)}_{\text{Self-Imitative}} + \underbrace{Q_\phi(\mathbf{z}_t, \pi_\theta(\cdot | \mathbf{z}_t)) - \alpha \mathcal{H}(\pi(\cdot | \mathbf{z}_t))}_{\text{Reinforcement Learning}} \right] \right]. \quad (4)$$

Here  $R_t = \sum_{t'=0}^T \gamma^{t'} r(s_t, \mathbf{a}_t)$  is the return of the whole trajectory and all the  $s_t, \mathbf{a}_t$  within this trajectory have the same return  $R_t$ . Compared to the original RL loss function, Another behavior cloning loss is introduced with the weight

$$\omega(R_t) = \beta \cdot \exp\left(\frac{R_t - G}{G}\right), \quad (5)$$

where  $G$  is a reference return value used to determine the level of the current return  $R_t$ . Ideally,  $G = R_{\text{target}}$  should be the target return, the standard for determining success or failure. However, this approach requires the introduction of additional prior information, which may affect the generality of the algorithm. Alternatively, we propose using the maximum return  $R_{\text{max}}$  of the trajectories in the current replay buffer as the reference standard.

### 3.3 Discussion and Analysis

From the implementation perspective, our proposed algorithm can be viewed as TD-MPC2 + BC, which might seem similar to the offline algorithm TD3+BC [Fujimoto and Gu, 2021]. However, the scenarios and problems they address are completely different. As an offline algorithm [Zhuang et al., 2023, Fujimoto et al., 2019, Kumar et al., 2020], TD3 + BC incorporates BC [Pomerleau, 1988] to prevent out-of-distribution (OOD) state-action pairs that lie beyond the offline dataset. In contrast, TDMPBC is a fully online algorithm that integrates imitation learning to accelerate exploration and learning within complex high-dimensional spaces.

Generally speaking, imitation learning [Zare et al., 2024] emphasizes exploitation and is a relatively conservative algorithm, whereas reinforcement learning places greater emphasis on exploration. TDMPBC can be regarded as a RL algorithm that incorporates conservatism. With the dynamic adjustment of BC weights, TDMPBC can be seen as a process where RL explores the space first, followed by rapid learning through imitation learning. The introduction of imitation learning does indeed carry the risk of causing the algorithm to converge to local optima. However, in the context of high-dimensional complex spaces such as humanoid robot motion control, converging to a local optimum like the upright posture is highly probable and often beneficial for downstream tasks.

## 4 Related Work

Behavior control for Humanoid robots is a long-standing problem, initially explored with simplified humanoid agent [Tunyasuvunakool et al., 2020] and recently with full-size humanoid robot [Zhuang et al., 2024a, Fu et al., 2024] such as Unitree H1. Humanoid robots are of particular interest to the reinforcement learning community because of the high-dimensional action space [Merel et al., 2017, Hansen et al., 2022a, 2023, 2024]. To overcome the challenges of exploration in high-dimensional action spaces, some algorithms learn policies by imitating human behavior [Fu et al., 2024] or enhance exploration through massive parallelization [Zhuang et al., 2024a]. In contrast, our proposed algorithm attempts to learn from scratch without the aid of massive parallelization [Makoviyuchuk et al., 2021]. We have extensively evaluated our algorithm on the HumanoidBench [Sferrazza et al., 2024], a benchmark built on humanoid robot with dexterous hands [Zakka et al., 2022] that contains not only 14 locomotion tasks but also 17 whole-body manipulation tasks. In the LocoMujoco [Al-Hafez et al., 2023], the H1 robot is not equipped with dexterous hands and only focus on locomotion tasks.

Confronted with tasks involving high-dimensional action spaces, model-based RL algorithms [Ha and Schmidhuber, 2018, Hansen et al., 2022a, Hafner et al., 2023, 2019] often prove to be more sample-efficient compared to model-free alternatives [Haarnoja et al., 2018, Fujimoto et al., 2018]. However, when it comes to humanoid robots with dexterous hands, even the SOTA model-based algorithms struggle to solve it [Sferrazza et al., 2024]. Our algorithm integrates the concept of imitation learning [Liu et al., 2023, Zhang et al., 2024] with the reinforcement learning framework, introducing a loss term of behavioral cloning [Pomerleau, 1988]. It may bear a resemblance to the offline RL [Zhuang et al., 2024b, Fujimoto et al., 2019] algorithm TD3+BC [Fujimoto and Gu, 2021] but our problem setting is completely different to theirs. Additionally, it should be noted that the SIRL framework is fundamentally an online RL paradigm that does not rely on expert data, different from IBRL [Hu et al., 2023] or MoDem [Hansen et al., 2022b].

## 5 Experiments

We evaluate our proposed TDMPBC in HumanoidBench [Sferrazza et al., 2024], which contains 14 locomotion tasks and 17 whole-body manipulation tasks. This benchmark is built on the Unitree H1 robot with dexterous hands, which has **151**-dimension observation space and **61**-dimension action space. Remarkably, this benchmark aims to evaluate online RL algorithms and does **not** include any expert demonstration. At the same time, SIRL is an improved online RL paradigm rather than imitation learning paradigm.

Specifically, the experiments cover the following five aspects of TDMPBC: **1)** Performance comparison with representative RL algorithms across 31 HumanoidBench tasks; **2)** The impact of the selection of hyperparameter  $\beta$  and reference return value  $G$ ; **3)** Increased runtime compared to TD-MPC2; **4)** The phenomenon of policy performance chasing the highest return in

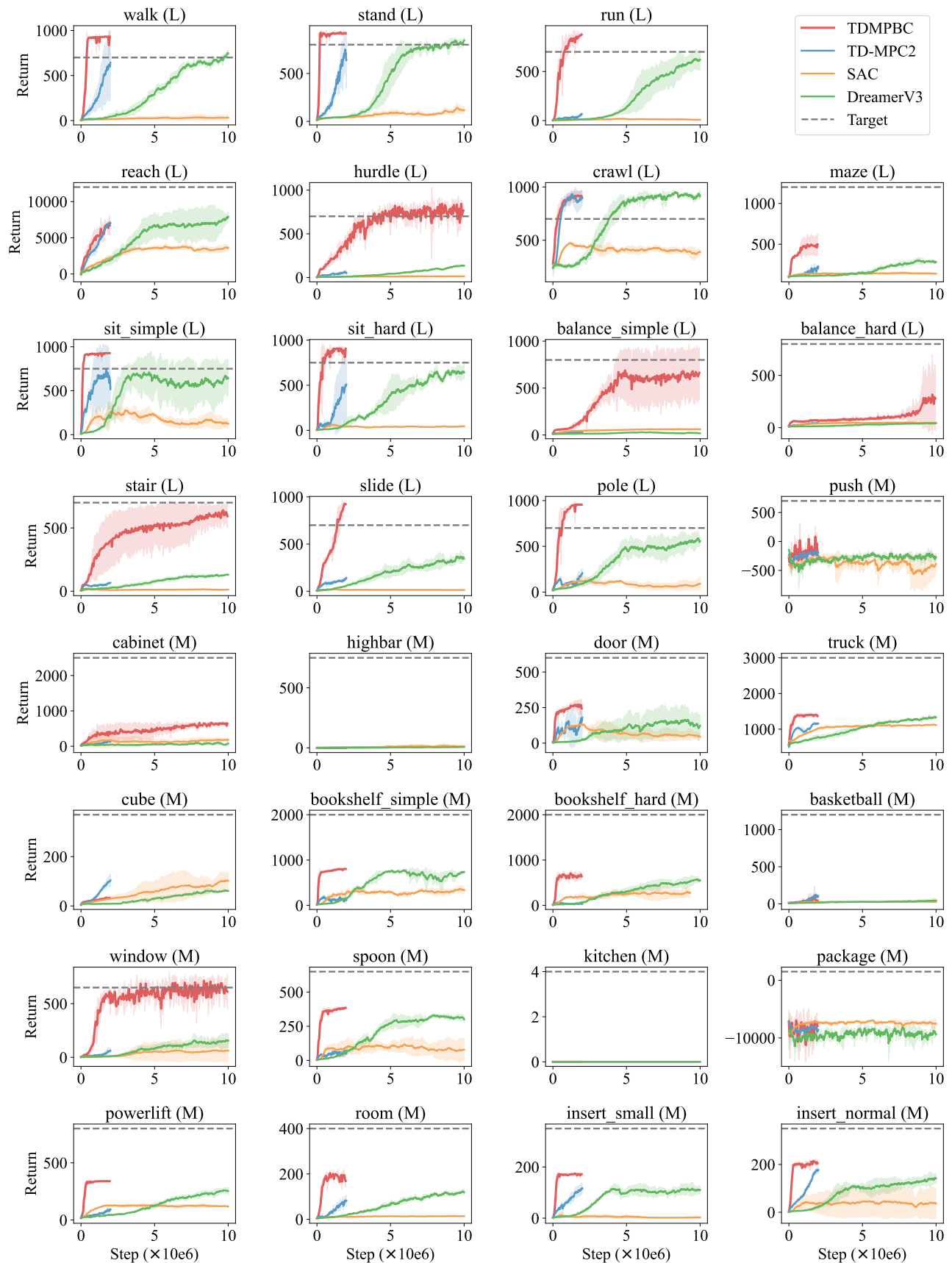


Figure 4: This figure presents the evaluation results on the HumanoidBench, where we conduct experiments with a total of three seeds and the shaded area representing one standard deviation. The baseline results are directly from the HumanoidBench.

the replay buffer during algorithm training; 5) Demonstration and analysis of some representative learned behaviors.

## 5.1 Performance Comparison

### 5.1.1 Baselines

We choose these three representative online reinforcement learning algorithms as our baselines:

- **SAC** (Soft Actor-Critic) [Haarnoja et al., 2018]: the state-of-the-art model-free off-policy RL algorithm with maximum entropy learning [Eysenbach and Levine, 2021];
- **DreamerV3** [Hafner et al., 2023]: the state-of-the-art model-based RL algorithm that learns from the imaginary model rollouts;
- **TD-MPC2** [Hansen et al., 2023]: the state-of-the-art model-based RL algorithm with online planning achieved via model predictive control (MPC).

As for on-policy algorithm PPO (Proximal Policy Optimization) [Schulman et al., 2017], its performance is inferior without the massive GPU parallelization so PPO is not our baseline.

In HumanoidBench, TD-MPC2 interacts with the environment for 2M steps, which takes approximately the same amount of time as SAC and DreamerV3 interacting for 10M steps. Therefore, the default training steps for TD-MPC2 are set to 2M, while others are set to 10M. Similarly, the default training steps for TDMPBC are also 2M. For tasks where performance significantly surpasses TD-MPC2 but still shows a clear upward trend without reaching the target, we choose to continue training up to 10M steps to demonstrate asymptotic performance. These environments include the `hurdle`, `balance_simple`, `balance_hard`, and `stair` tasks in Locomotion, as well as the `cabinet` and `window` tasks in Whole-body Manipulation.

### 5.1.2 Results on Locomotion

HumanoidBench contains a total of 14 locomotion tasks, corresponding to the first 14 training curves ending with (L) in Figure 4. It should be noted that, while the locomotion tasks can be accomplished without dexterous hands, the H1 robot here is indeed equipped with dexterous hands. The entire robot has **151**-dimensional observations (51 dimension for body and 50 dimension for each hand), plus a **61**-dimensional action space, which is quite challenging for RL control. TDMPBC achieves significantly faster convergence and higher final performance compared to the baseline in all environments except for `reach` and `crawl`. More importantly, TDMPBC surpasses the target (represented by the grey dashed line) in 8 tasks, indicating successful task completion. In contrast, the baselines are only capable of completing the `crawl` task.

### 5.1.3 Results on Whole-Body Manipulation

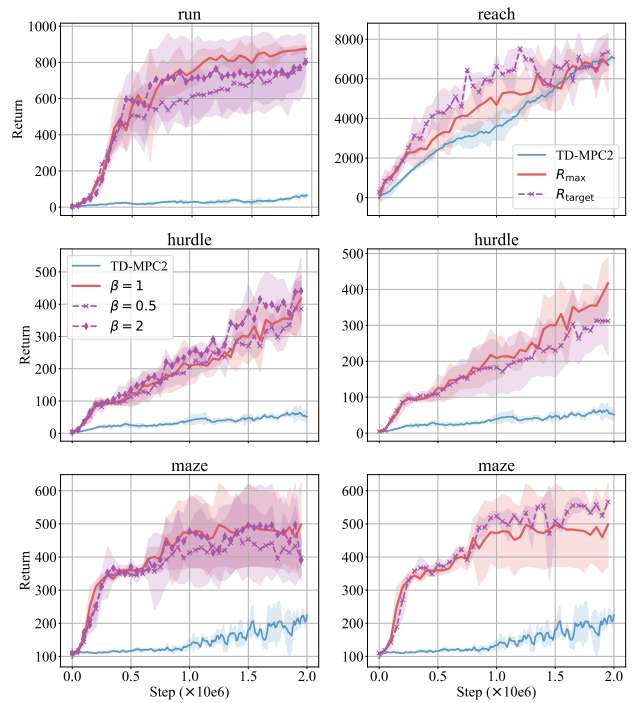
HumanoidBench contains a total of 17 whole-body manipulation tasks, corresponding to the last 17 training curves ending with (M) in Figure 4. Whole-body manipulation requires not

only the control of body posture but also the operation of dexterous hands to accomplish grasping. Although our algorithm has achieved obvious improvements, the final results are still far behind the target return. Our algorithm also struggles to simultaneously control the body and achieve dexterous hand grasping. A prematurely converging curve implies that the humanoid rapidly masters one thing while the other one fails.

## 5.2 Ablation Study

### 5.2.1 Ablation on hyperparameter $\beta$

The  $\beta$  balances the original reinforcement learning and our proposed self-imitative behavior cloning in policy loss function Equation 4. Due to the presence of the exponential function and  $R_t \leq G$ , the range of behavior cloning item is between  $(0, 1]$ . Meanwhile, Q is obtained by discrete regression in a log-transformed space, which means the Q has been normalized [Hafner et al., 2023]. Due to the same scale between RL loss and behavior cloning loss, the default value of hyperparameter is  $\beta = 1$ . In Section 5.1, the experimental results are presented for the case where  $\beta = 1$ . To further investigate the robustness of TDMPBC, we conducted additional control experiments with  $\beta = 0.5$  and  $\beta = 2.0$ . We found that the performance of TDMPBC is highly robust to values of  $\beta$  around 1.



(a) Ablation on  $\beta$  (b) Ablation on  $G$

Figure 5: The left figures illustrate the impact of different hyperparameter values ( $\beta = 0.5, 1.0, 2.0$ ) on the performance of TDMPBC across three tasks: `run`, `hurdle`, and `maze`. The right figures demonstrate the effects of two different goal settings ( $G = R_{\max}$  and  $G = R_{\text{target}}$ ) on the performance of TDMPBC across three tasks: `reach`, `hurdle`, and `maze`.

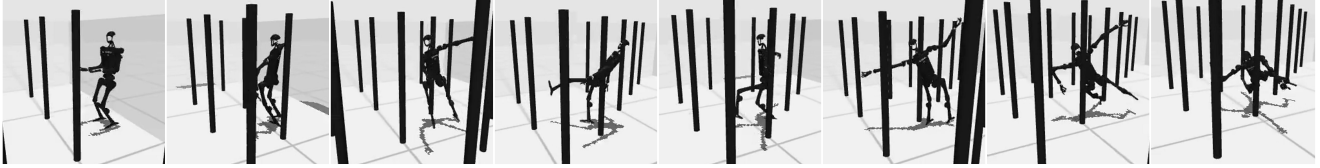


Figure 6: The visualization of baseline TD-MPC2 on the pole task. The robot collides with the pole and falls to the ground.

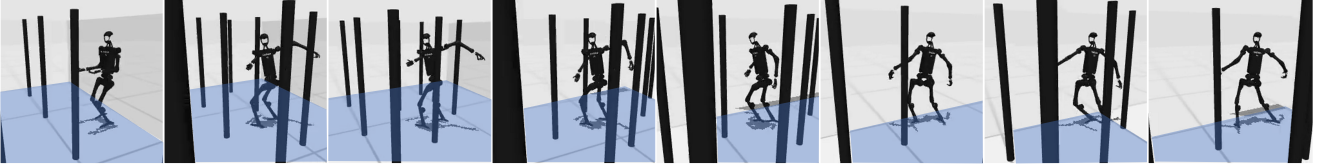


Figure 7: The visualization of our TDMPBC on the pole task. To avoid collisions, the robot chooses to stay close to the wall, thereby passing through quickly and stably. The ground is marked in blue to more clearly illustrate the moving toward the wall.

### 5.2.2 Ablation on reference return value $G$

The  $G = R_{\text{target}}$  of the current task serves as a globally optimal benchmark but necessitates the introduction of additional information. In contrast, the maximum return  $G = R_{\text{max}}$  in the current replay buffer represents the upper limit achievable by the current policy, which grows in tandem with the policy’s performance as training progresses. Meanwhile,  $G = R_{\text{target}}$  functions more as a pre-established, relatively higher objective. In Figure 5, we found no significant differences in overall performance between the two. Therefore, we opted for  $G = R_{\text{max}}$  to avoid incorporating prior information. It is also worth noting that in tasks where the return can exceed the target,  $G = R_{\text{max}}$  may ultimately surpass  $G = R_{\text{target}}$ .

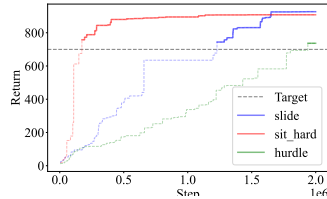


Figure 8: Gradually,  $R_{\text{max}}$  may potentially exceed  $R_{\text{target}}$ .

### 5.3 Runtime

Compared to TD-MPC2, TDMPBC introduces only a marginal increase in computational burden for policy loss calculations and requires the replay buffer to additionally store the current maximum return value. We measure the time required to run three seeds simultaneously on a Tesla V100-SXM2-32G GPU across three different tasks in Table 1. When the GPU is upgraded to an NVIDIA A100-SXM4-40GB, the time can be further reduced to approximately 20 hours. On average, TDMPBC only increases the time by less than 5%, yet achieved a remarkable performance improvement of over 120%.

Table 1: A comparison of the runtime of our proposed algorithm TDMPBC and the baseline TD-MPC2 on the same hardware.

Tasks	TDMPBC	TD-MPC2	Improvement
walk	37.71 ± 0.13	35.23 ± 0.38	+ 7.06%
reach	37.73 ± 0.64	36.46 ± 0.71	+ 3.48%
hurdle	36.61 ± 0.06	35.34 ± 0.13	+ 3.61%
<b>Average</b>	<b>37.35 (h)</b>	<b>35.68 (h)</b>	<b>+ 4.72%</b>

### 5.4 Training phenomenon

In the experiments, we observed that the return obtained by evaluating the current policy is often lower than the maximum return in the replay buffer, regardless of whether it is our proposed TDMPBC or the baseline algorithm TD-MPC2 in Figure 9. Intuitively, it appears as though the policy is constantly chasing the current maximum return, and the behavior cloning (BC) in SIRL accelerates this.

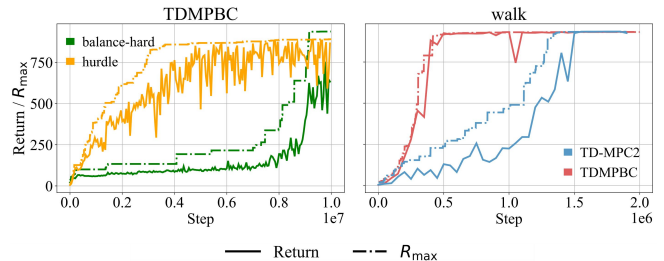


Figure 9: The curves of the policy’s return (solid line) and the maximum return in the current replay buffer (dashed line) during training. The left figure shows these curves for TDMPBC on the balance-hard and hurdle tasks, while the right figure compares the curves for TDMPBC and TD-MPC2 on the walk.

### 5.5 Behavior Visualization

In this subsection, we present representative behaviors obtained from TDMPBC, including the pole and balance-hard tasks in locomotion, as well as the window task in whole-body manipulation.

pole: In the pole task, the humanoid robot is required to navigate forward through a dense forest of tall, slender poles without collision. The robot trained with TD-MPC2 continuously collides with the poles and is unable to move forward properly, eventually falling over. Once step inside the pole forest, the robot swiftly moves towards one of the side walls. It then proceeds to hug the wall, keep escaping the dense poles, thereby avoiding potential collisions. This clever avoidance strategy, closely resembling human behavior, is exactly the reason our algorithm converges rapidly.

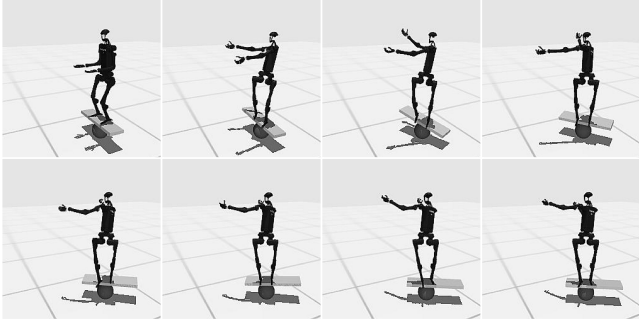


Figure 10: The visualization of our TDMPBC on the `balance-hard` task, where the humanoid robot aims to maintain balance on an unstable board, with the spherical pivot beneath the board in motion.

`balance_hard`: The humanoid robot is required to maintain balance on an unstable plank, beneath which lies a movable sphere. Upon initialization, the robot nearly falls backward but manages to stabilize itself by swinging its arms, ultimately achieving a balanced posture. During this process, the sphere is displaced from the center of the plank to a position slightly to the left.

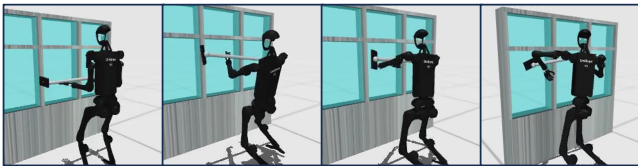


Figure 11: The visualization of our TDMPBC on the `window` task, where the humanoid aims to grab a window wiping tool and keep its tip parallel to a window by following a prescribed vertical speed.

`window` : For the window task, the robot should ideally use its dexterous hands to control the cleaning tools. However, the robot does not master the control of its dexterous hands and instead chooses to press against the cleaning surface with its arms to complete the task. Despite the algorithm achieving a high return on this task, it does not perform the task as expected.

## 6 Conclusion, Limitation and Future Work

In this paper, we propose the Self-Imitative Reinforcement Learning (SIRL) framework to accelerate the online learning of humanoid robots. We have made a simple yet effective modification to TD-MPC2 by incorporating a behavior cloning (BC) loss term into the policy training loss function. Our proposed algorithm has demonstrated significant performance improvements in the HumanoidBench with a little additional computation overhead. Current research has achieved remarkable progress in locomotion tasks, yet there remains substantial room for improvement in whole-body manipulation. Looking ahead, we plan to transition TDMPBC from simulated environments to real-world deployment, further exploring its strengths and weaknesses.

## References

- Andrea Bonci, Pangcheng David Cen Cheng, Marina Indri, Giacomo Nabissi, and Fiorella Sibona. Human-robot perception in industrial environments: A survey. *Sensors*, 21(5):1571, 2021.
- Olivier Stasse and Thomas Flayols. An overview of humanoid robots technologies. *Biomechanics of Anthropomorphic Systems*, pages 281–310, 2019.
- Avishek Choudhury, Huiyang Li, Christopher Greene, and Sunanda Perumalla. Humanoid robot-application and influence. *arXiv preprint arXiv:1812.06090*, 2018.
- Carmelo Sferrazza, Dun-Ming Huang, Xingyu Lin, Youngwoon Lee, and Pieter Abbeel. Humanoidbench: Simulated humanoid benchmark for whole-body locomotion and manipulation. *arXiv preprint arXiv:2403.10506*, 2024.
- Jan Peters, Sethu Vijayakumar, and Stefan Schaal. Reinforcement learning for humanoid robotics. In *Proceedings of the third IEEE-RAS international conference on humanoid robots*, pages 1–20, 2003.
- David Silver, Aja Huang, Chris J Maddison, Arthur Guez, Laurent Sifre, George Van Den Driessche, Julian Schrittwieser, Ioannis Antonoglou, Veda Panneershelvam, Marc Lanctot, et al. Mastering the game of go with deep neural networks and tree search. *nature*, 529(7587):484–489, 2016.
- David Silver, Julian Schrittwieser, Karen Simonyan, Ioannis Antonoglou, Aja Huang, Arthur Guez, Thomas Hubert, Lucas Baker, Matthew Lai, Adrian Bolton, et al. Mastering the game of go without human knowledge. *nature*, 550(7676):354–359, 2017.
- Julian Schrittwieser, Ioannis Antonoglou, Thomas Hubert, Karen Simonyan, Laurent Sifre, Simon Schmitt, Arthur Guez, Edward Lockhart, Demis Hassabis, Thore Graepel, et al. Mastering atari, go, chess and shogi by planning with a learned model. *Nature*, 588(7839):604–609, 2020.
- Matteo Hessel, Joseph Modayil, Hado Van Hasselt, Tom Schaul, Georg Ostrovski, Will Dabney, Dan Horgan, Bilal Piot, Mohammad Azar, and David Silver. Rainbow: Combining improvements in deep reinforcement learning. In *Proceedings of the AAAI conference on artificial intelligence*, volume 32, 2018.
- Takahiro Miki, Joonho Lee, Jemin Hwangbo, Lorenz Wellhausen, Vladlen Koltun, and Marco Hutter. Learning robust perceptive locomotion for quadrupedal robots in the wild. *Science robotics*, 7(62):eabk2822, 2022.
- Joonho Lee, Jemin Hwangbo, Lorenz Wellhausen, Vladlen Koltun, and Marco Hutter. Learning quadrupedal locomotion over challenging terrain. *Science robotics*, 5(47):eabc5986, 2020.
- Jemin Hwangbo, Joonho Lee, Alexey Dosovitskiy, Dario Belluscio, Vassilios Tsounis, Vladlen Koltun, and Marco Hutter. Learning agile and dynamic motor skills for legged robots. *Science Robotics*, 4(26):eaau5872, 2019.
- Nicklas Hansen, Hao Su, and Xiaolong Wang. Td-mpc2: Scalable, robust world models for continuous control. *arXiv preprint arXiv:2310.16828*, 2023.

- Danijar Hafner, Jurgis Pasukonis, Jimmy Ba, and Timothy Lillicrap. Mastering diverse domains through world models. *arXiv preprint arXiv:2301.04104*, 2023.
- Nicklas Hansen, Xiaolong Wang, and Hao Su. Temporal difference learning for model predictive control. *arXiv preprint arXiv:2203.04955*, 2022a.
- Richard S Sutton, Andrew G Barto, et al. Introduction to reinforcement learning. 1998.
- Tuomas Haarnoja, Aurick Zhou, Pieter Abbeel, and Sergey Levine. Soft actor-critic: Off-policy maximum entropy deep reinforcement learning with a stochastic actor. In *International conference on machine learning*, pages 1861–1870. PMLR, 2018.
- Grady Williams, Andrew Aldrich, and Evangelos Theodorou. Model predictive path integral control using covariance variable importance sampling. *arXiv preprint arXiv:1509.01149*, 2015.
- Maryam Zare, Parham M Kebria, Abbas Khosravi, and Saeid Nahavandi. A survey of imitation learning: Algorithms, recent developments, and challenges. *IEEE Transactions on Cybernetics*, 2024.
- Dean A Pomerleau. Alvin: An autonomous land vehicle in a neural network. *Advances in neural information processing systems*, 1, 1988.
- Scott Fujimoto and Shixiang Shane Gu. A minimalist approach to offline reinforcement learning. *Advances in neural information processing systems*, 34:20132–20145, 2021.
- Zifeng Zhuang, Kun Lei, Jinxin Liu, Donglin Wang, and Yilang Guo. Behavior proximal policy optimization. *arXiv preprint arXiv:2302.11312*, 2023.
- Scott Fujimoto, David Meger, and Doina Precup. Off-policy deep reinforcement learning without exploration. In *International Conference on Machine Learning*, pages 2052–2062. PMLR, 2019.
- Aviral Kumar, Aurick Zhou, George Tucker, and Sergey Levine. Conservative q-learning for offline reinforcement learning. *Advances in Neural Information Processing Systems*, 33: 1179–1191, 2020.
- Saran Tunyasuvunakool, Alistair Muldal, Yotam Doron, Siqi Liu, Steven Bohez, Josh Merel, Tom Erez, Timothy Lillicrap, Nicolas Heess, and Yuval Tassa. dm\_control: Software and tasks for continuous control. *Software Impacts*, 6:100022, 2020.
- Ziwen Zhuang, Shenzhe Yao, and Hang Zhao. Humanoid parkour learning. *arXiv preprint arXiv:2406.10759*, 2024a.
- Zipeng Fu, Qingqing Zhao, Qi Wu, Gordon Wetzstein, and Chelsea Finn. Humanplus: Humanoid shadowing and imitation from humans. *arXiv preprint arXiv:2406.10454*, 2024.
- Josh Merel, Yuval Tassa, Dhruva TB, Sriram Srinivasan, Jay Lemmon, Ziyu Wang, Greg Wayne, and Nicolas Heess. Learning human behaviors from motion capture by adversarial imitation. *arXiv preprint arXiv:1707.02201*, 2017.
- Nicklas Hansen, Jyothir SV, Vlad Sobal, Yann LeCun, Xiaolong Wang, and Hao Su. Hierarchical world models as visual whole-body humanoid controllers. *arXiv preprint arXiv:2405.18418*, 2024.
- Viktor Makoviychuk, Lukasz Wawrzyniak, Yunrong Guo, Michelle Lu, Kier Storey, Miles Macklin, David Hoeller, Nikita Rudin, Arthur Allshire, Ankur Handa, et al. Isaac gym: High performance gpu-based physics simulation for robot learning. *arXiv preprint arXiv:2108.10470*, 2021.
- Kevin Zakka, Yuval Tassa, and MuJoCo Menagerie Contributors. MuJoCo Menagerie: A collection of high-quality simulation models for MuJoCo, 2022. URL [http://github.com/google-deepmind/mujoco\\_menagerie](http://github.com/google-deepmind/mujoco_menagerie).
- Firas Al-Hafez, Guoping Zhao, Jan Peters, and Davide Tateo. Locomujoco: A comprehensive imitation learning benchmark for locomotion. *arXiv preprint arXiv:2311.02496*, 2023.
- David Ha and Jürgen Schmidhuber. Recurrent world models facilitate policy evolution. *Advances in neural information processing systems*, 31, 2018.
- Danijar Hafner, Timothy Lillicrap, Jimmy Ba, and Mohammad Norouzi. Dream to control: Learning behaviors by latent imagination. *arXiv preprint arXiv:1912.01603*, 2019.
- Scott Fujimoto, Herke Hoof, and David Meger. Addressing function approximation error in actor-critic methods. In *International conference on machine learning*, pages 1587–1596. PMLR, 2018.
- Jinxin Liu, Li He, Yachen Kang, Zifeng Zhuang, Donglin Wang, and Huazhe Xu. Ceil: Generalized contextual imitation learning. *Advances in Neural Information Processing Systems*, 36:75491–75516, 2023.
- Ziqi Zhang, Jingzhe Xu, Zifeng Zhuang, Jinxin Liu, et al. Context-former: Stitching via latent conditioned sequence modeling. *arXiv preprint arXiv:2401.16452*, 2024.
- Zifeng Zhuang, Dengyun Peng, Ziqi Zhang, Donglin Wang, et al. Reinformer: Max-return sequence modeling for offline rl. *arXiv preprint arXiv:2405.08740*, 2024b.
- Hengyuan Hu, Suvir Mirchandani, and Dorsa Sadigh. Imitation bootstrapped reinforcement learning. *arXiv preprint arXiv:2311.02198*, 2023.
- Nicklas Hansen, Yixin Lin, Hao Su, Xiaolong Wang, Vikash Kumar, and Aravind Rajeswaran. Modem: Accelerating visual model-based reinforcement learning with demonstrations. *arXiv preprint arXiv:2212.05698*, 2022b.
- Benjamin Eysenbach and Sergey Levine. Maximum entropy rl (provably) solves some robust rl problems. *arXiv preprint arXiv:2103.06257*, 2021.
- John Schulman, Filip Wolski, Prafulla Dhariwal, Alec Radford, and Oleg Klimov. Proximal policy optimization algorithms. *arXiv preprint arXiv:1707.06347*, 2017.

## A Contributions

The first version of this paper is completed by the following five authors: Zifeng Zhuang\*, Diyuan Shi\*, Ting Wang, Shangke Lyu and Donglin Wang. The first version was submitted to ICRA (about **2024.9**), but it was desk-rejected due to formatting issues. Zifeng Zhuang\* proposes and leads the entire project. Diyuan Shi\* develops the code and conducts all the experiments, and thus is credited as a co-first author. Dr. Ting Wang implements the policy evaluation and visualization, participates in the writing of the paper and provides valuable feedback. Dr. Shangke Lyu provides extensive discussions on article structure, which ensures the smooth progress of the entire project. Professor Donglin Wang fully supports the development of this project, provides all the necessary resources.

In the second version of the paper (current version), three additional authors contributed including Runze Suo, Xiao He and Hongyin Zhang. Runze Suo implements the modification of weights and update the code. Xiao He participates in data preprocessing and visualization of the paper. Hongyin Zhang offers numerous valuable suggestions for the writing of the paper.

## B HumanoidBench

HumanoidBench [Sferrazza et al., 2024] is a comprehensive simulated humanoid robot benchmark designed to evaluate and advance research in whole-body locomotion and manipulation tasks. It aims to provide a standardized platform for testing and developing algorithms for humanoid robots, addressing the challenges of complex dynamics, sophisticated coordination, and long-horizon tasks.

**A.1 Simulated Humanoid Robot:** HumanoidBench features a humanoid robot equipped with two dexterous hands, specifically the Unitree H1 robot with Shadow Hands. The robot is simulated using the MuJoCo physics engine, which provides fast and accurate physics simulation. The environment supports both position control and torque control, with the action space normalized to  $[-1, 1]$  for 61 actuators (19 for the body and 21 for each hand).

**A.2 Tasks** HumanoidBench includes a diverse set of 31 tasks, divided into 14 locomotion tasks and 17 whole-body manipulation tasks. These tasks range from simple locomotion (e.g., walking, running) to complex manipulation (e.g., package unloading, tool usage, furniture assembly). Below is the specific list of tasks:

### Locomotion tasks

- **Walk:** The robot maintains a velocity of approximately 1 m/s, ensuring it does not fall to the ground.
- **Stand:** The robot maintains a standing pose.
- **Run:** The robot maintains a velocity of approximately 5 m/s, ensuring it does not fall to the ground.
- **Reach:** The robot’s left hand reaches a randomly initialized 3D point.
- **Hurdle:** The robot maintains a velocity of approximately 5 m/s while clearing hurdles, ensuring it does not fall to the ground.
- **Crawl:** The robot traverses through a tunnel at a velocity of approximately 1 m/s.
- **Maze:** In a maze, the robot reaches its target location by making multiple turns at intersections.
- **Sit:** In *sit\_simple*, the robot sits on a chair located nearby behind it. The *sit\_hard* task involves a movable chair, where the robot sits on a chair positioned at random directions and locations.
- **Balance:** The robot maintains its balance on an unstable board. In *balance\_simple*, the spherical pivot beneath the board remains stationary, whereas in *balance\_hard*, the pivot is mobile.
- **Stair:** The robot ascends and descends stairs at a velocity of 1 m/s.
- **Slide:** The robot slides upwards and downwards at a velocity of 1 m/s.
- **Pole:** The robot advances through a dense forest composed of high thin poles, without colliding with them.

### Whole-Body Manipulation tasks

- **Push:** The robot moves a box to a randomly initialized 3D point on a table.
- **Cabinets:** The robot opens four different types of cabinet doors (such as hinged doors, sliding doors, drawers, and pull-up cabinets) and performs various pick-and-place manipulations inside the cabinets.
- **Highbar:** The robot maintains a grip with both hands on the high bar, swinging while maintaining its hold until it reaches a vertical, upside-down position.

- **Door:** The robot turns the doorknob to open the door, and walks through it while keeping the door open.
- **Truck:** The robot unloads packages from a truck onto a platform.
- **Cube:** The robot manipulates a cube with each hand, aligning both cubes with specific, randomly initialized target orientations.
- **Bookshelf:** The robot rearranges five objects on a bookshelf, which is equivalent to five designated sub-tasks, each involving the positioning of a different object to a target location. The sub-tasks must be completed in order. In *bookshelf\_simple*, the order of sub-tasks is always the same, whereas in *bookshelf\_hard*, the order is randomized.
- **Basketball:** The robot catches a ball coming from a random direction and throws it into the basket.
- **Window:** The robot, holding a window cleaning tool, maintains its tip parallel to the window while adhering to a specified vertical velocity.
- **Spoon:** The robot picks up a spoon located next to a pot and uses it to draw circles in the pot.
- **Kitchen:** The robot performs a series of actions in a kitchen environment, including opening the microwave door, moving a kettle, turning a burner, and switching on and off the lights.
- **Package:** The robot moves a box to a randomly initialized target location.
- **Powerlift:** The robot lifts a barbell of a designed mass.
- **Room:** The robot arranges a 5m by 5m room, minimizing the positional variance in the x and y axes by filling it with randomly dispersed objects.
- **Insert:** The robot inserts the ends of a rectangular block into two small pegs. *Insert\_small* and *insert\_normal* indicate different object sizes.

**A.3 Observation and Action Space** The observation space for the robot state includes joint positions and velocities, totaling 151 dimensions (49 for the body and 51 for each hand). Additionally, the environment provides task-specific observations, such as object positions and velocities, to facilitate interaction with the environment. The action space is normalized to  $[-1, 1]$  for 61 actuators, which includes 19 actuators for the humanoid body and 21 actuators for each hand. The action space is designed to be consistent across all tasks to minimize domain-specific tuning.

## C Experimental Details

We implemented our TDMPBC algorithm on the source code of TD-MPC2 in HumanoidBench <https://github.com/carlosferrazza/humanoid-bench>. The parameters used were the default parameters of HumanoidBench when running TD-MPC2. For the additional hyperparameter  $\beta$  that we introduced, it was set to  $\beta = 1$  in all experiments.

## D More Experiment Results

More experiment results are presented here. Figure 12 compares the evaluation curves of our proposed TDMPBC against the baseline TD-MPC2, while Table 2 provides a summary of performance across various methods on HumanoidBench tasks, effectively demonstrating the efficacy of our approach.

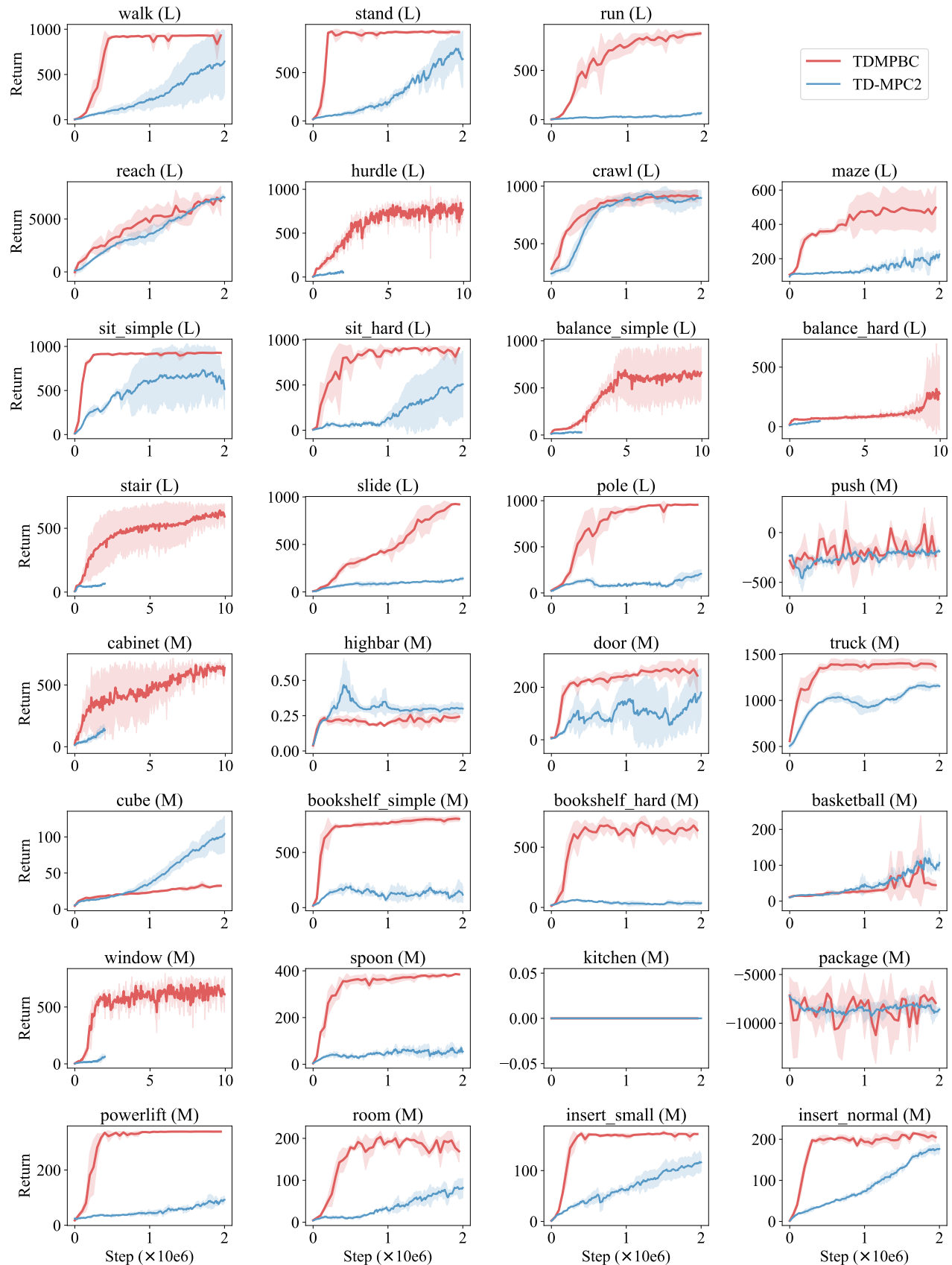


Figure 12: The evaluation curves of our proposed TDMPBC and the baseline TD-MPC2. We conduct experiments with a total of three seeds and the shaded area representing one standard deviation.

Table 2: Summary of Results for HumanoidBench Tasks. In the results, non-target-exceeding scores are displayed in gray, and the best results for each task are highlighted in **bold**.

Tasks	Target	TDMPBC@2M	TD-MPC2@2M	DreamerV3@10M	SAC@10M
walk	700	<b>932.08 ± 0.82</b>	644.19 ± 344.25	751.02 ± 28.25	36.40 ± 30.28
stand	800	<b>929.67 ± 0.69</b>	749.79 ± 133.86	845.36 ± 33.43	141.98 ± 56.35
run	700	<b>874.58 ± 21.69</b>	66.14 ± 9.97	629.33 ± 81.75	18.36 ± 3.30
reach	12000	7013.83 ± 685.29	7120.75 ± 253.64	<b>7926.20 ± 546.66</b>	3800.29 ± 344.43
hurdle	700	<b>843.54 ± 63.58</b>	64.68 ± 9.70	137.46 ± 9.07	13.85 ± 8.90
crawl	700	920.54 ± 45.88	<b>931.69 ± 33.19</b>	<b>950.98 ± 10.38</b>	471.95 ± 12.13
maze	1200	<b>497.66 ± 124.50</b>	224.62 ± 25.65	301.77 ± 36.47	149.40 ± 13.84
sit_simple	750	<b>928.82 ± 1.12</b>	733.90 ± 255.79	710.96 ± 208.93	275.94 ± 33.41
sit_hard	750	<b>908.75 ± 2.27</b>	508.98 ± 365.77	662.55 ± 22.79	61.06 ± 13.78
balance_simple	800	<b>688.86 ± 239.99</b>	34.07 ± 4.42	29.89 ± 0.27	62.61 ± 2.73
balance_hard	800	<b>317.27 ± 379.72</b>	48.18 ± 8.49	45.04 ± 6.13	50.82 ± 2.56
stair	700	<b>640.37 ± 46.99</b>	66.50 ± 6.77	132.14 ± 1.80	18.02 ± 4.91
slide	700	<b>926.26 ± 2.17</b>	141.30 ± 19.09	367.61 ± 37.71	19.65 ± 7.25
pole	700	<b>958.58 ± 1.11</b>	207.46 ± 43.65	589.01 ± 74.35	123.30 ± 49.65
push	700	<b>83.54 ± 164.92</b>	-168.50 ± 45.46	-144.62 ± 73.83	-263.98 ± 54.44
cabinet	2500	<b>664.13 ± 14.69</b>	147.62 ± 34.00	105.45 ± 52.28	183.28 ± 63.76
highbar	750	0.26 ± 0.05	0.47 ± 0.19	7.58 ± 2.11	<b>18.43 ± 20.10</b>
door	600	<b>270.92 ± 30.80</b>	179.83 ± 91.33	165.83 ± 104.86	131.79 ± 12.89
truck	3000	<b>1402.91 ± 49.02</b>	1164.00 ± 38.29	1341.04 ± 33.58	1128.40 ± 16.26
cube	370	33.79 ± 4.65	104.14 ± 25.21	63.57 ± 2.83	<b>104.34 ± 32.21</b>
bookshelf_simple	2000	<b>805.64 ± 25.83</b>	194.37 ± 33.46	773.76 ± 33.82	363.68 ± 71.15
bookshelf_hard	2000	<b>707.57 ± 45.21</b>	64.19 ± 3.07	577.13 ± 60.55	300.05 ± 97.77
basketball	1200	111.83 ± 126.20	<b>120.66 ± 21.77</b>	46.22 ± 26.74	34.10 ± 10.00
window	650	<b>714.22 ± 37.04</b>	63.27 ± 19.87	158.37 ± 68.57	65.68 ± 107.28
spoon	650	<b>386.39 ± 0.64</b>	70.69 ± 23.39	331.83 ± 11.30	118.28 ± 47.47
kitchen	4	0.00 ± 0.00	0.00 ± 0.00	0.00 ± 0.00	0.00 ± 0.00
package	1500	-6957.24 ± 1154.91	-7228.07 ± 467.74	-8124.26 ± 337.79	<b>-6946.94 ± 30.56</b>
powerlift	800	<b>339.15 ± 0.22</b>	92.48 ± 11.16	260.93 ± 24.58	128.70 ± 9.52
room	400	<b>203.53 ± 13.99</b>	84.20 ± 17.95	123.92 ± 10.52	14.50 ± 0.18
insert_small	350	<b>174.47 ± 4.34</b>	117.24 ± 21.27	115.93 ± 18.22	11.87 ± 13.05
insert_normal	350	<b>214.55 ± 4.12</b>	176.66 ± 10.58	144.09 ± 18.02	47.00 ± 67.78